Synthesis and Characterization of Electrically Conducting Copolymers Based on Biphenyl and Thiophene

Johannis Simitzis, Despina Triantou, Spyridon Soulis

Department III "Materials Science and Engineering," Laboratory Unit "Advanced and Composite Materials," School of Chemical Engineering, National Technical University of Athens, Athens 157 73, Greece

Received 20 December 2009; accepted 14 March 2010
DOI 10.1002/app.32493
Published online 3 June 2010 in Wiley InterScience (www.interscience.wiley.com).

ABSTRACT: New electrically conducting copolymers based on biphenyl and thiophene in a form of film were synthesized by electropolymerization using potentiostatic conditions and the corresponding homopolymers, polyphenylenes, and polythiophenes, for comparison reasons. Different values of applied potential were used, to study its effect on the structure, morphology, and electrical conductivity of the films. From the analysis of the current-time curves, it was found that the growth of the films follows layer by layer (2D) mechanism. The films were studied by FTIR, TGA, XRD, SEM-EDAX and their electrical conductivity was determined, as well as their energy gap (E_g) by cyclic voltammetry. The copolymers had higher conductivity (appr. 1 S/cm) and lower E_g (appr. 1.2 eV) than that of the corresponding homopolymers. These materials due to their high conductivity, high stability under repetitive potential cycling, and partial solubility are candidates for electronic applications. © 2010 Wiley Periodicals, Inc. J Appl Polym Sci 118: 1494–1506, 2010

Key words: conducting polymers; polyphenylene; polythiophene; copolymerization; electrical conductivity; nucleation and growth mechanism

INTRODUCTION

Conducting polymers (CPs) were first produced in the mid-1970s as a novel generation of organic materials that have electrical properties similar to those of metals or inorganic semiconductors and simultaneously they exhibit the attractive properties of conventional polymers, such as ease of synthesis and flexibility in processing.[1,2] CPs are used in areas such as rechargeable batteries,[3–5] electroluminescent polymer displays,[3] polymer light-emitting diodes,[3–5] flexible "plastic" transistors,[3] sensors,[4,6,7] and photovoltaic cells.[4,5]

CPs can be synthesized by chemical polymerization or by electropolymerization, whereas the latter offers several advantageous features,[1,3,5] such as absence of catalyst, direct formation of the doped polymer film on the electrode surface, easy control of the film thickness and the possibility of performing *in situ* characterization of the deposited film by electrochemical and other techniques.[3,5] Polyphenylenes are one of the most important classes of conjugated polymers and have been the subject of extensive research, particularly as active materials for use in light-emitting diodes (LEDs) and polymer lasers. These materials have been of particular interest as potential blue emitters in such devices.[8,9] Polyphenylenes can be prepared using benzene or other aromatic compounds, such as biphenyl, leading to poly(*p*-phenylene)s, PPP, or to isomeric polyphenylenes, PP, respectively.[10] PPP contains only para-couplings and is an infusible and insoluble polymer, however PP contains ortho-, meta-, and para-couplings and is more processable than PPP.[11] Polythiophene and its derivatives based on heterocyclic monomers are another important class of CPs[3,4] and they are stable in air and moisture both in doped and undoped states.[12,13]

Apart from the conducting homopolymers, copolymers based on different types of monomers have gained great scientific interest, because new electrically active materials could be produced having characteristic properties of both of the homopolymers.[14,15] By electrochemical copolymerization, a variety of conducting materials with different electrical and morphological properties can be produced.[14,15] In the literature, the copolymerization of biphenyl with 3-octylthiophene has been studied, to produce soluble copolymers.[14–17] Moreover, the polymerization of 2-biphenyl-3-octylthiophene (BOT), has been reported, to produce poly(2-biphenyl-3-octylthiophene) (PBOT).[18,19] Compared to thiophene, 3-octylthiophene and BOT are quite expensive reagents, thus it could be cost effective to study whether copolymers of thiophene with biphenyl could lead to materials with combination of desirable properties (e.g. higher conductivity and better thermal stability than the homopolymers). The aim of this work is to copolymerize biphenyl with

Correspondence to: J. Simitzis (simj@chemeng.ntua.gr).

thiophene by electropolymerization to produce electrically conducting films. Their structure, morphology, thermal stability, and electrical conductivity will be examined in comparison to that of the corresponding homopolymers.

EXPERIMENTAL

Thiophene (Th, Fluka) was vacuum distilled before use. Tetrabutylammonium tetrafluoroborate ($TBABF_4$, Merck) was dried at 110°C up to constant weight. Acetonitrile (ACN, Merck, water content ~ 0.05 %) was stored over molecular sieves (Fluka, 4 Å, 8–12 mesh) for about one month. Biphenyl (Biph, Fluka) was used as received.

The copolymer films based on Biph and Th and the corresponding homopolymers were synthesized by anodic potensiostatic electropolymerization at various constant potentials for 30 min. The electropolymerization solution consisted of the monomers (Biph and/or Th), $TBABF_4$ as supporting electrolyte and ACN as solvent. The monomers were used with concentrations: [Biph]/[Th] = 0.05*M*/0.05*M* for copolymers, [Biph] = 0.1*M* for polyphenylene homopolymers and [Th] = 0.1*M* for polythiophene homopolymers and the electrolyte concentration was [$TBABF_4$] = 0.1*M*. All electropolymerizations took place at room temperature, in one-compartment electrochemical cell of 150 mL volume using a system of three electrodes. The latter includes the working and the counter electrodes, both of Pt-plated Pt in the form of plates (with surface area of 4.8 and 9.0 cm^2, respectively) and the calomel electrode (SCE) as reference, placed into Luggin capillary.[14,20] Before electropolymerization, the surface of the working electrode was cleaned by heating over a flame to remove residues. The electropolymerization solution was deoxygenated by bubbling nitrogen for 10 min before the beginning of the electropolymerization. The corresponding apparatus was a Potentioscan Wenking POSS88 (Bank Elektronik). The thickness of the films synthesized was estimated from the amount of charge during the electropolymerization. After polymerization, the films synthesized were immersed in acetonitrile to remove $TBABF_4$ residues and the soluble oligomers and then were vacuum dried at 30°C up to constant weight.

The solubility of the films synthesized was tested in various common solvents (i.e. ethanol, methanol, acetone, *N*-methylpyrrolidone, tetrahydrofuran, *N*,*N*′ diemethylformamide, chlorobenzene, *N*,*N*′ dimethylsulfoxide etc.). The FTIR spectra of the polymers were recorder using a PerkinElmer Spectrum GX spectrometer using KBr discs. The TGA measurements were recorded using a Mettler Toledo 815E thermobalance with aluminum pans, by heating the sample from 25°C up to 1000°C with a heating rate of 10°C/min, under nitrogen flow. The morphology of the films was examined using a FEI Quanta 200 Scanning Electron Microscope with simultaneous Energy Dispersive X-Ray Analysis (EDAX). The degree of crystalinity, x_c (%) of the polymers was determined from their XRD diffractograms, recorded on a Siemens D5000 diffractometer, with CuKa radiation and scan rate of 0.02 degrees per second. The electrical conductivity of the films with constant current was determined at room temperature by the two-probe technique.[21] The energy levels of the Highest Occupied Molecular Orbital (E_{HOMO}) and that of Lowest Unoccupied Molecular Orbital (E_{LUMO}), as well as the energy gap (E_g), were determined by cyclic voltammetry (CV, Potentioscan Wenking POSS88, Bank Elektronik), in a 0.1*M* $TBABF_4$ solution in ACN, using the previously described electrochemical cell. The film (as deposited film on the electrode) was placed in the solution and underwent cyclic potential sweep, firstly from 0 to –2 V and then from 0 to +2 V (scan rate: 100 mV/s).[22,23]

RESULTS AND DISCUSSION

Synthesis of polymer films

To synthesize the copolymer films, the oxidation potential (E_{ox}) of the combination of the monomers should be known, as this is the minimum potential where copolymerization could take place. The E_{ox} was determined by oxidative scanning of an electopolymerization solution (acetonitrile containing $TBABF_4$ and monomers at the same concentrations as that used for the synthesis of the films) from 0 V up to +3 V vs SCE with a scan rate of 100 mV/s. From the current (i) – potential (E) curve the E_{ox} was determined as the potential where the current increases abruptly.[24,25] Specifically, for the biphenyl–thiophene monomer system, E_{ox} = 1.80 V (vs SCE). The available literature E_{ox} values of biphenyl[10,20] and thiophene[26] for similar electropolymerization solutions were experimentally confirmed without deviations as 1.80 and 1.65 V (vs SCE), respectively.

To investigate the effect of applied potential on the properties of the films, electropolymerizations were carried out at potentials up to 0.1 V higher than E_{ox}, with an increase step of 0.02 V. For example, copolymers of Biph with Th were synthesized at 1.80 (E_{ox}), 1.82, 1.84, 1.86, 1.88, and 1.90 V (vs SCE). The synthesized films were macroscopically examined and those that were inhomogeneous were discarded. It should be noted that the results of the electrical conductivity were in accordance with those of the macroscopic observation, i.e. the films that were inhomogeneous had lower electrical conductivity. Thus, from this point on, only the films

TABLE I
Raw Materials, Experimental Parameters, Total Charge, and Characteristics (thickness, color) of Synthesized Polymeric Films

Code of polymers		Raw materials: Monomers: Biphenyl (mol/L)	Raw materials: Monomers: Thiophene (mol/L)	Experimental parameters: Applied potential for 30 min (V vs SCE)	Total charge (mC/cm^2)	Characteristics of films synthesized: Thickness (μm)	Characteristics of films synthesized: Color
(1)		(2)	(3)	(4)	(5)	(6)	(7)
Homopolymers	Copolymers						
$PP_{1.80}$		0.1	–	1.80	821.63	5.75	Dark brown
$PP_{1.82}$				1.82	796.91	5.58	Dark brown
$PP_{1.84}$				1.84	578.04	4.04	Dark brown
$PTh_{1.71}$		–	0.1	1.71	1475.57	3.69	Black
$PTh_{1.73}$				1.73	1551.34	3.88	Black
$PTh_{1.75}$				1.75	1227.46	3.07	Black
	$(PP\text{-}PTh)_{1.80}$	0.05	0.05	1.80	1803.26	8.57	Black
	$(PP\text{-}PTh)_{1.82}$			1.82	1688.85	8.02	Black
	$(PP\text{-}PTh)_{1.84}$			1.84	2085.87	9.91	Black

Supporting electrolyte: Tetrabutylenamonium tetrafluoroborate ($TBABF_4$), 0.1*M*.
Solvent: Acetonitrile (ACN).

synthesized under the chosen potentials (which lead to homogeneous films) will be considered.

Table I presents the raw materials, the experimental parameters, the total charge and the characteristics (thickness, color) of synthesized polymeric films. Based on the presentation of Figure 1, the total charge and the thickness of films can be determined. This figure shows the current (i) – time (t) curves for the electropolymerization of the representative homopolymers $PP_{1.80}$, $PTh_{1.71}$, and copolymer $(PP\text{-}PTh)_{1.84}$. By integrating the surface below the (i)–(t) curve, the corresponding charge (Q) during the electropolymerization was determined (Table I, column 5). The thickness of a certain film was estimated from the corresponding charge.[27,28] According to literature,[28] the synthesis of a polyphenylene film with thickness of 1 μm requires 142.8 mC/cm^2 (Q_{PP}), whereas that of polythiophene requires 400 mC/cm^2 (Q_{PTh}).[29] Given that there are no relative information concerning the copolymers of biphenyl and thiophene, it was assumed that the charge required for the synthesis of a 1 μm thick copolymer film ($Q_{PP\text{-}PTh}$) corresponds to the harmonic mean of Q_{PP} and Q_{PTh}:

$$Q_{PP\text{-}PTh} = (2 * Q_{PP} * Q_{PTh})/(Q_{PP} + Q_{PTh}) \quad (1)$$

Thus, $Q_{PP\text{-}PTh} = 210.5\ mC/cm^2$. The thickness of the copolymer films is greater than that of the homopolymer films (Table I, column 6). The polyphenylene films synthesized had dark brown color, whereas polythiophene and copolymers films had black (Table I, column 7).

Electropolymerization mechanism

Before the analysis of (i)–(t) curves, the electropolymerization mechanism should be described. In the case of biphenyl (Scheme 1), a radical is formed initially (a) by the protonation of the monomer.[27,30] This radical, after the loss of a proton and subsequent oxidation, forms the radical cation (b). Then, this radical cation can be coupled with a monomer molecule or with another radical cation. In biphenyl the first mechanism dominates (c) and thus the radical cation of the dimer is formed. The latter, after the loss of a proton and subsequent oxidization (d), leads to the formation of a dimer. With the same reactions the polymer chain keeps on growing. The polymer deposition onto the electrode surface begins

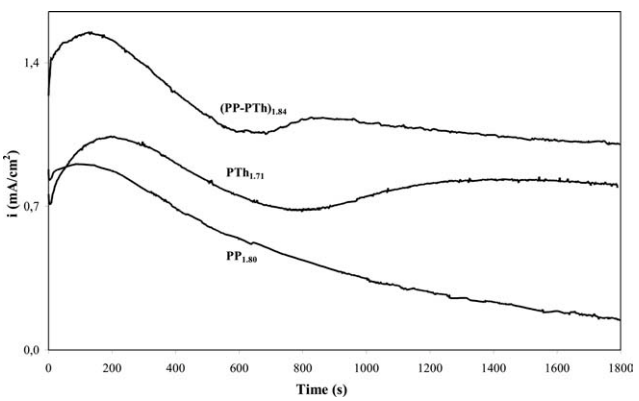

Figure 1 Current versus electropolymerization time for homopolymers $PP_{1.80}$, $PTh_{1.71}$, and copolymer $(PP\text{-}PTh)_{1.84}$ (for the codes, see Table I).

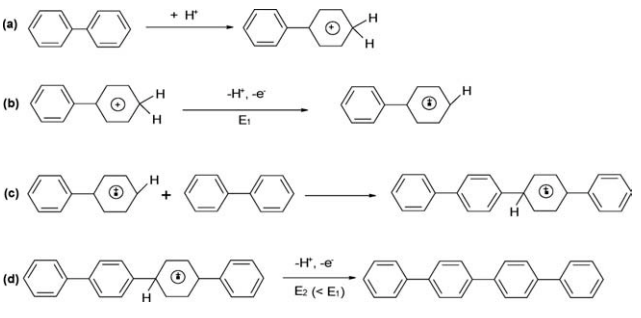

Scheme 1 Mechanism of biphenyl electropolymerization.[13]

when the oligomers formed reach the critical chain length that makes them insoluble in the electropolymerization solution.[3,10,12,31,32] In the case of the electropolymerization of thiophene (Scheme 2), the first step is the same as that of biphenyl, i.e. the formation of a radical cation (a). This radical cation can be coupled with a monomer molecule or with another radical cation and, contrarily to biphenyl, in thiophene the second mechanism dominates and a dihydrodimer dication (b) is formed. The latter, after losing two protons and re-aromatizing, leads to the dimer (c). Due to the potential applied the dimer, which is more easily oxidized than the monomer, reacts to form its radical cation (d) and the latter is coupled with the radical cation of the monomer (e). Then, it loses two protons and rearomatizes, this way forming the trimer (f).[3,5,10,12,31,32] With the same reactions, the polymer chain keeps on growing.

According to Figure 1, the shape of the (*i*)–(*t*) curve of polyphenylene differs significantly from that of polythiophene. The corresponding curve of the copolymer resembles that of polythiophene. Based on the literature,[10,33–41] the basic reaction steps take place between $t = 0$ s and $t = 300$ s. Therefore, the initial part of the (*i*)–(*t*) curve of the homopolymer $PP_{1.82}$ is presented in Figure 2(a) and the whole curve in Figure 2(b). Similarly, the initial part of the (*i*)–(*t*) curve of the copolymer $(PP\text{-}PTh)_{1.84}$ is presented in Figure 3(a) and the whole curve in Figure 3(b). As shown below, the experimental curves are separated in to the following Regions, taking into consideration the literature[10,33–41]:

Region I

Before the initiation of electropolymerization, there is an interface between the working electrode and the electrolytic solution. When a voltage is applied on the cell, the abrupt response is attributed to the charging of the interface.[33,34,37] After charging, the current decreases due to the monomer(s) adsorption onto the interface and its oxidation to radical cation (Scheme 1, case a and b and Scheme 2, case a). Usually, this adsorption is controlled by diffusion.[33,34,37] The duration of this region is less than 40 s and its end indicates the initiation of the nucleation.

Region II

When nucleation initiates, a gradual increase of the current is observed.[10,34–36,39] Specifically, in this region two radical cations (which were formed during Region I) are bonded together (Scheme 2, case b) or a radical cation with a monomer (Scheme 1, case c). Following the progress of the reaction, oligomers are formed containing 2 to 5 aromatic rings (Scheme 1 case d and Scheme 2, cases c and f). According to the literature, this region is less than 100 s[10] and its end can be graphically determined from the point where the initial steep rate decreases.[10,33,34,36]

Region III (III_a and III_b)

In this region, the current continues to increase (Region III_a) but with smaller rate than that of Region II, indicating the continuation of the growth of the already mentioned nuclei.[10,35,36] After a certain time, the growth rate is stabilized and the film is formed, resulting to a current plateau (Region III_b).[34]

Region IV (IV_a, IV_b, and IV_c)

This region refers to macroscopic phenomena, since the film has been formed and its growth continues.

Subregion IV_a

In this subregion the current decreases due to the decrease of the film growth rate. This decrease of

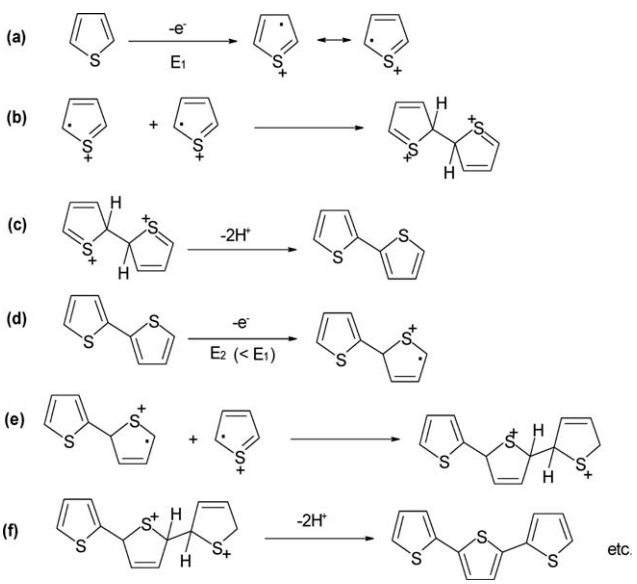

Scheme 2 Mechanism of thiophene electropolymerization.[5]

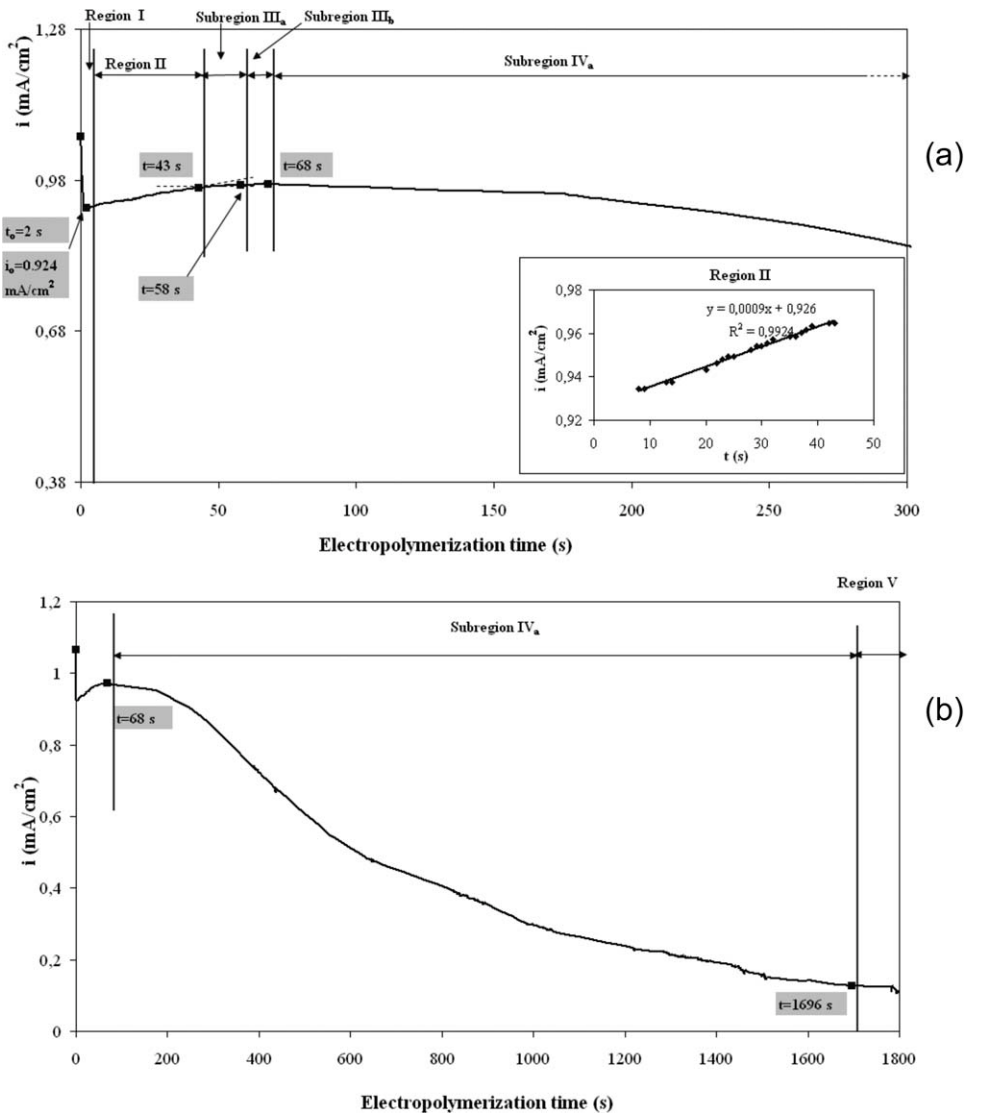

Figure 2 Current versus electropolymerization time for homopolymer $PP_{1.82}$, (for the code, see Table I). (a) Time from 0 up to 300 s. (b) Time from 300 up to 1800 s.

the rate is the result of two different factors: (1) the overlapping of the growing nuclei which decrease the active surface of the electrode[33] and (2) a considerable amount of the radical cations formed in the region near to the electrode diffuse to the electrolytic solution and they do not take part to the film growth.[37]

Subregion IV_b

During this subregion the current increases. The current increase indicates the formation of a new phase, i.e. a new kind of polymer is deposited. In the literature,[38,39] in a similar current increase, it has been reported that two different films were deposited in two definite phases. It is considered that the different phases of polymer growth result to the deposition of two layers with different structure. The strongly adhered to the electrode and compact initial layer is followed by a thicker, loosely adhered layer. The initial layer has higher density compared to that of the thicker layer deposited later on. The second phase of polymer formation follows an exponential relation of current versus time, which is indicative of a one dimension polymer growth, with continuous branches.[40] The formation of two different polymer layers may be attributed to the different degree of monomer oxidation in the electrode surface compared to that in the surface of the already formed film.

Subregion IV_c

In this subregion, the current decreases, after its increase in IV_b. This decrease is due to the decrease of the growth rate of the second polymer layer (i.e. that with the branches).[36,39]

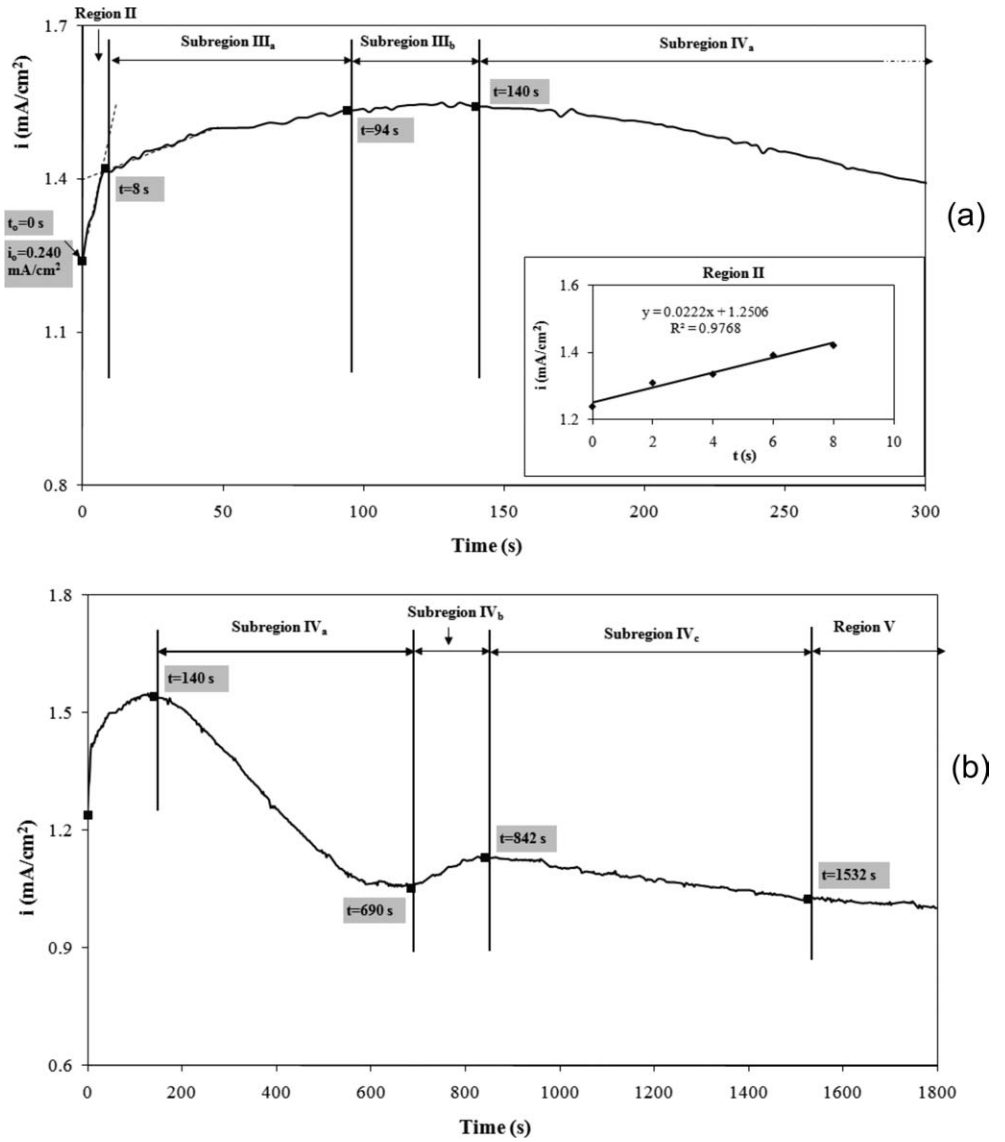

Figure 3 Current versus electropolymerization time for copolymer $(PP\text{-}PTh)_{1.84}$, (for the code, see Table I). (a) Time from 0 up to 300 s (b) Time from 300 up to 1800 s.

Region V

The current reaches an almost constant value, indicating that the film growth follows a steady rate.[34,36,41] The time where the current reaches constant value depends on the applied potential and as a general rule it decreases with increasing applied potential.[41]

Table II shows the time limits of the above described Regions of the synthesized polymers. Polyphenylenes generally do not exhibit the Subregions IV_b and IV_c. Polythiophenes exhibit generally all Regions. Copolymers do not exhibit Region I. Subregion IV_b is undesirable, given that it leads to inhomogeneous films. This Subregion appeared in the case of $PTh_{1.71}$, $PTh_{1.75}$, and $(PP\text{-}PTh)_{1.84}$ but it was narrow and did not affect the uniformity of the films (as macroscopically observed).

The nucleation and growth mechanism (NGM) can be determined from the analysis of Region II in the (i)–(t) curves. There are three criteria for the NGM: (a) instantaneous (IN) or progressive (P), (b) one (1D), two (2D), or three (3D), dimensional nucleation and (c) controlled by diffusion or charge transfer. Depending on the type of NGM, the current follows a power-type relationship with time. The type of NGM can be determined from the plot of (i) versus t^x, where x: $-(1/2)$, $(1/2)$, 1, 2, 3, and $(3/2)$, finding which superscript gives linear relationship in respect to current.[33,36–38] In polyphenylenes $x = 1$ [inset of Fig. 2(a)], indicating that the NGM is instantaneous, two-dimensional nucleation (IN2D), controlled by charge transfer.[33] In polythiophenes $x = (1/2)$, indicating that the NGM is IN2D controlled by diffusion with interactions between the growing centers (nuclei).[33] The same superscript ($x = 1/2$) is

TABLE II
Time Limits of Regions Based on Current-Time Curves of the Polymers

	Time limits (in s) of regions and subregions based on (*i*)–(*t*) curves							
			III		IV			
Code of polymers	I	II	IIIa	III_b	IV_a	IV_b	IV_c	V
$PP_{1.80}$	0–2	3–20	21–85	86–141	142–1800	–	–	–
$PP_{1.82}$	0–2	3–43	44–58	59–68	69–1696	–	–	1697–1800
$PP_{1.84}$	0–4	5–19	–	20–38	39–1655	–	–	1666–1800
$PTh_{1.71}$	0–8	9–24	25–150	151–234	235–822	823–1290	–	1291–1800
$PTh_{1.73}$	0–6	7–38	39–182	183–394	395–1800	–	–	–
$PTh_{1.75}$	0–10	11–38	39–116	117–260	261–944	945–1048	1049–1800	–
$(PP\text{-}PTh)_{1.80}$	–	0–8	9–149	150–540	541–1800	–	–	–
$(PP\text{-}PTh)_{1.82}$	–	0–6	7–152	153–336	337–1690	–	–	1691–1800
$(PP\text{-}PTh)_{1.84}$	–	0–8	9–94	95–140	141– 690	691–842	843–1532	1533–1800

determined for most of the copolymers, except from $(PP\text{-}PTh)_{1.84}$ where $x = -(1/2)$, indicating that the NGM is IN2D controlled by diffusion but with no interactions between the growing centers.[33] Consequently, the growth of homopolymer and copolymer films takes place in two dimensions (2D) as layer by layer, i.e. growing only in parallel direction.[33] This way of growth is very important for the quality of the films, as it leads to compact film, contrarily to 3D growth (not observed in the films synthesized) that leads to loose, powder like-films.[33]

Structural characterization of the copolymers

Figure 4 shows the FTIR spectra of the copolymer $(PP\text{-}PTh)_{1.84}$ and, for comparison, that of the homopolymers $PP_{1.82}$, $PTh_{1.71}$. The various bands of the copolymers and the homopolymers were attributed to chemical bonds according to the literature for the polyphenylenes[10,20,42–45] and polythiophenes[30,46–50] and they are summarized in Table III. The bands at 1600, 1570, 1500, 1480, nd 1400 cm^{-1} are associated with the aromatic ring. The broad absorption band at 1600 cm^{-1} is particularly strong if a further conjugation with aromatic rings takes place. Based on the literature,[51,52] the band at 1570 cm^{-1} is attributed to quinoid structures and the band at 1480 cm^{-1} to benzenoid structures. Moreover, the copolymers exhibit the bands of various C—H vibrations at 1085 and 1030 cm^{-1} ("in plane" bending vibrations), at 875 and 805 cm^{-1} ("out of plane" bending vibrations), at 765 cm^{-1} (bending vibrations) and at 695 cm^{-1} (deformation vibrations). Additionally, they exhibit the band of C—S bending vibrations at 610 cm^{-1}.[49] The latter is characteristic of the thiophene structural unit.

In polyphenylenes, the type of substitution can be obtained from the intense bands below 900 cm^{-1}.[10,42] The band at $\sim$ 805 cm^{-1} is characteristic of the para-substitution and the bands at 765 cm^{-1} and 695 cm^{-1} are characteristic of the aromatic rings, which are at the end of the macromolecules, i.e. (mono) end-groups. In the case of the presence of the bands at 880–870 cm^{-1}, the stronger bands at 765 cm^{-1} and 695 cm^{-1} can be attributed to meta-substitution. The small band at 740 cm^{-1} indicating ortho-substitution is absent from the spectra.[10,42] Thus, all the synthesized polyphenylenes exhibit para- and meta-substitution. Polythiophenes exhibit the bands at 1499–1490 and 800–790 cm^{-1}, that indicate the growth of the polymer chain in α,α′-direction (α,α′-coupling), characteristic of 2,5-polythiophene.[48–50] On the other hand, the peaks at 830–825 and 730 cm^{-1} of α, β coupling (i.e. 2,4-polythiophene)[46,47] are not present. Thus, the synthesized polythiophenes were exclusively 2,5-polythiophene.

Concerning the FTIR spectra of the copolymers, their absorption bands cannot confirm that the films synthesized were indeed copolymers, as the characteristic bands of the homopolymers appear in the same regions and thus they overlap. The only band that could be used as a criterion is that of C—S, but it appears near the low limit of the spectra (at 615 cm^{-1}). To confirm that the films formed were copolymers, the solubility of the homopolymers and the copolymers was tested in various common solvents. PPs were totally soluble in *N*-methylpyrrolidone and totally insoluble in all other solvents tested, whereas PThs were totally insoluble in all the solvents tested. Copolymers are partially soluble in tetrahydrofuran

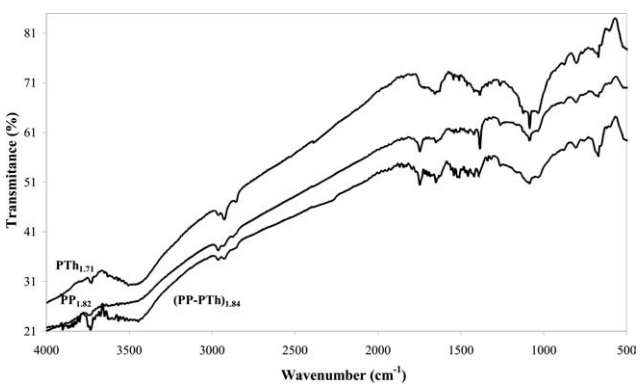

Figure 4 FTIR spectra of homopolymers $PP_{1.82}$, $PTh_{1.71}$, and copolymer $(PP\text{-}PTh)_{1.84}$ (for the codes, see Table I).

TABLE III
Description of FTIR Bands of Homopolymers and Copolymers

Characteristic bonds	Wavenumber according to literature[10,20,30,42–50] (cm^{-1})	Homopolymers						Copolymers		
		Polyphenylenes			Polythiophenes					
		$PP_{1.80}$	$PP_{1.82}$	$PP_{1.84}$	$PTh_{1.71}$	$PTh_{1.73}$	$PTh_{1.75}$	$(PP\text{-}PTh)_{1.80}$	$(PP\text{-}PTh)_{1.82}$	$(PP\text{-}PTh)_{1.84}$
$>CH_2$: aliphatic (cyclic and linear) parts	2980–2950	2955	2951	*n*	2956	2961	2956	*n*	*n*	2960
		2919	2924	2915	2915	2916	2924	*n*	*n*	2915
	2890–2850	2860	2853	*n*	2846	2845	2847	*n*	*n*	*n*
C=O: bending vibrations	1740–1710	1731	1743	–	1727	1732	1728	1738	1738	1765
C=C: stretching vibrations of aromatic ring	1600	Broad band 1652	1629	1635	1638	1635	1639	1638	1625	1640
	1570	1567	1580	1572	1563	1563	1570	1564	1563	1569
	1530	–	–	–	1530	1532	1532	*n*	*n*	–
	1499–1490	1500	1505	1510	1490	1491	1492	1510	1508	1505
	1460	–	–	–	1470	1463	1460	–	–	–
C–C bending vibrations of aromatic ring	1480	1482	1475		1476	1407	1477	1480	1480	1484
	1400	1381	1384	–	1384	1384	1384	*n*	1385	1390
C–H "in plane" bending vibrations	1150–1110	1168	–	1137	1113	1117	1116	–	–	–
	1094–1000	Broad band 1081–982	1082	1081	1082	1084	1083	1083	1084	1083
				1028	1025	1032	1033	1030	1025	1029
C–H: "out of plane" bending vibrations, characteristic of separated H in aromatic ring	876	874	*n*	870	874	874	875	867	*n*	876
C–H: "out of plane" bending vibrations of two neighboring H in aromatic ring	805	805	801	807	800	800	790	801	802	801
C–H: bending vibrations of four or five neighboring H in aromatic ring	765	755	*n*	752	764	763	764	762	764	*n*
o-substitution in benzene ring	740	738	–	*n*	–	–	–	–	–	–
CH_2: aliphatic (cyclic and linear) parts	722	–	–	–	714	714	712	–	–	–
C–H: deformation vibrations "out of plane" in aromatic ring	695	693	682	694	698	696	695	697	*n*	670
					670	670	671	670		
C–S bending vibrations	615	–	–	–	609	615	617	617	610	610

n: Negligible.

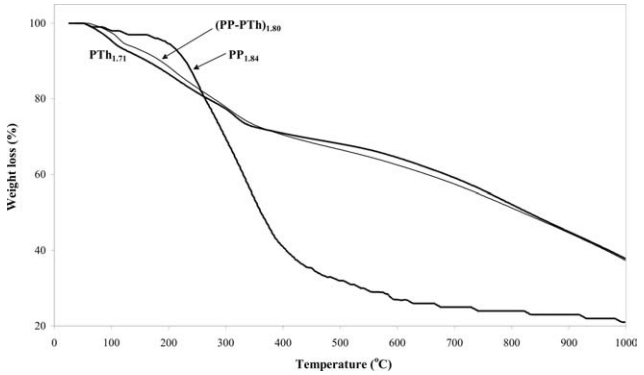

Figure 5 TGA curves of homopolymers $PP_{1.84}$, $PTh_{1.71}$, and copolymer $(PP\text{-}PTh)_{1.80}$ (for the codes see Table I).

and totally insoluble in all other solvents tested. Specifically, the soluble fraction of the copolymers $(PP\text{-}PTh)_{1.80}$, $(PP\text{-}PTh)_{1.82}$, and $(PP\text{-}PTh)_{1.84}$ is 20, 23, and 30%, respectively. This different solubility behavior of the copolymers indicates that their structure differs from that of the homopolymers.

Based on the XRD the polyphenylenes synthesized are totally amorphous, opposite to the polythiophenes which have crystallinity, x_c (%), i.e. 6.5, 15.0, and 30.3% for $PTh_{1.71}$, $PTh_{1.75}$, and $PTh_{1.73}$, respectively. The copolymers $(PP\text{-}PTh)_{1.80}$ and $(PP\text{-}PTh)_{1.82}$ have crystallinity, x_c (%), i.e. 27.8 and 19.4%, respectively, opposite to $(PP\text{-}PTh)_{1.84}$, which is amorphous.

Thus, x_c (%) of the copolymers follows the order:

$$(PP-PTh)\,1.80 > (PP-PTh)\,1.82 > (PP-PTh)\,1.84,$$

i.e. the increase of the applied potential of the electropolymerization leads to the production of less crystalline or amorphous copolymers. The order of crystallinity of the copolymers is in accordance with their insoluble in tetrahydrofuran fraction, following the general relation between crystallinity and solubility.

Figure 5 shows the TGA curves of the homopolymers $PP_{1.84}$, $PTh_{1.71}$ and the copolymer $(PP\text{-}PTh)_{1.80}$. $PP_{1.84}$ is almost stable up to 200°C and then up to 600°C exhibits an abrupt weight loss (73% of its initial weight). On the other hand, the weight loss of $PTh_{1.71}$ begins at lower temperature (50°C) and continues up to 1000°C with an almost steady rate. As a result, $PTh_{1.71}$ has much lower weight loss above 300°C than $PP_{1.84}$. The copolymer $(PP\text{-}PTh)_{1.80}$ has a weight loss behavior similar to that of $PTh_{1.71}$. The weight loss of the polymers can be analyzed in three regions: the first up to 200°C, the second up to 500°C and the final up to 1000°C, as it is shown in Table IV that includes also the total weight loss.

From the TGA results, the structure of the copolymer can be established. If the copolymer contained separate large segments of homopolymer PP and homopolymer PTh (resembling a block copolymer), then it would have been stable up to 200°C and would have had an abrupt weight loss at approximately 300°C, due to the decomposition of the large segments of PP. Thus, the copolymer macromolecules contain distributed monomeric units of biphenyl and thiophene. Therefore, there are not meta-linkages between the monomeric units of biphenyl. The high weight loss of $PP_{1.84}$ above 200°C is a prove that it contains not only para-, but also meta-linkages between biphenyl units. Indeed, poly (paraphenylene) having only para-linkages, exhibits a very low weight loss (undoped: 25%, doped: 40% up to 1000°C).[42] Consequently, the disadvantage of meta-linkages of biphenyl units does not appear in the macromolecules of the copolymers and the latter follows a similar thermal degradation like $PTh_{1.71}$.

Morphology and elemental analysis of the copolymers

Figure 6 presents the SEM micrographs of copolymers and homopolymers. In Figure 6(a), $PP_{1.80}$ has a globular morphology with aggregates with size between 3.5 and 6 μm. $PP_{1.84}$, Figure 6(b), has a sponge-like structure with small size aggregates (smaller than 1 μm), but it appears more compact than $PP_{1.80}$. Polythiophene films $PTh_{1.71}$ and $PTh_{1.75}$, Figure 6(c,d), have a fibrillar structure with round shaped pores. $PTh_{1.71}$ has smaller pores (with diameter 8–10 μm) than $PTh_{1.75}$ (with diameter 10–12 μm). The copolymer $(PP\text{-}PTh)_{1.80}$, Figure 6(e), has round shaped cracks, but appears compact. Specifically, it has a few large sized cracks (with diameter 12–16 μm) and other significantly smaller (with diameter 3–7 μm). The copolymer $(PP\text{-}PTh)_{1.84}$, Figure 6(f) has a totally different morphology, with many, large

TABLE IV
Weight Loss (%) of the Polymers for Different Temperature Ranges According to TGA

Code of polymers	Weight loss (%) for temperature ranges			Total weight loss (%)
	25–200°C	200–500°C	500–1000°C	
$PP_{1.84}$	6.0	62.5	10.5	79.0
$PTh_{1.71}$	13.4	18.5	30.3	62.2
$(PP\text{-}PTh)_{1.80}$	11.5	22.0	29.2	62.7

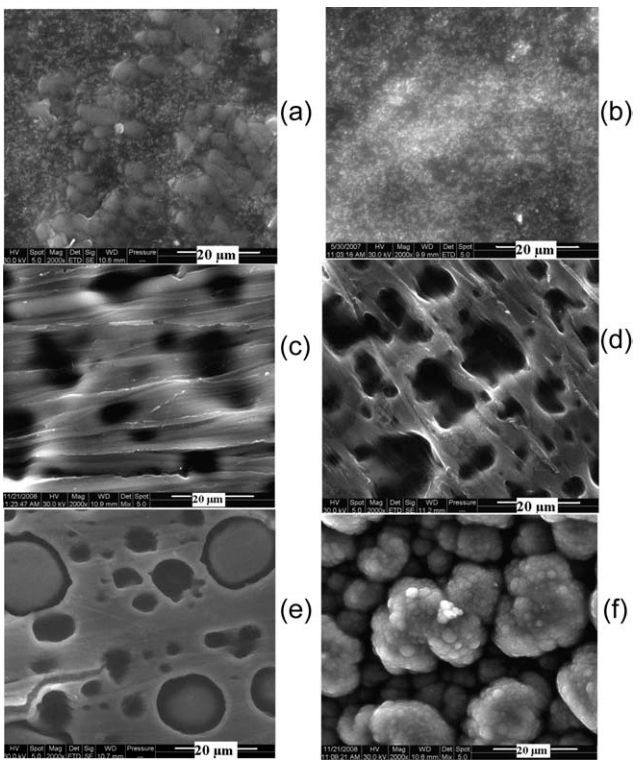

Figure 6 SEM micrographs (× 2000) of (a), (b) homopolymer $PP_{1.80}$, $PP_{1.84}$, respectively, (c), (d) homopolymer $PTh_{1.71}$, $PTh_{1.75}$, respectively (e), (f) copolymer $(PP\text{-}PTh)_{1.80}$, $(PP\text{-}PTh)_{1.84}$, respectively (for the codes see Table I).

sized (12–19 μm) aggregates of cauliflower shape. The different morphology of the copolymers confirms that the potential of electropolymerization has a strong influence on the film formation and its structure. The copolymers have very different morphology compared to the homopolymers, indicating that they are indeed copolymers.

Based on the elemental analysis from EDAX data, the ratio of structural unit of homopolymers per BF_4^- dopant ion (counter ion) was calculated, Table V. For polyphenylenes, the ratio of F/C (w/w) was converted to the molecular ratio of F/C and then (taking into consideration that a dopant anion contains 4 fluorine atoms) in BF_4^-/C (mol/mol). The latter ratio can be converted to the ratio of structural biphenyl units per counter ion, taking into consideration that one structural biphenyl unit contains 12 carbon atoms. Similarly, the ratio of structural thiophene units (containing one sulfur atom) per counter ion was calculated. For polyphenylenes, it was found that the ratio is between 4.4 ($PP_{1.84}$) and 5 ($PP_{1.80}$) structural units per dopant ion. For polythiophenes, it was found that this ratio is between 3.6 ($PTh_{1.71}$) and 3.8 ($PTh_{1.73}$) structural units per dopant ion, which are in accordance with corresponding values in the literature for p-doping of polythiophenes.[3]

For the copolymers, the ratio of structural unit derived from biphenyl per that derived from thiophene was calculated[15] and the values are presented in Table V. For this calculation, only the amounts of carbon and sulfur are necessary, thus the amounts of oxygen and fluorine were omitted and the ratio of carbon to sulfur was expressed in percentage rate (% w/w). This ratio was converted to molecular ratio (mol/mol) and then the structural units of biphenyl and thiophene contained into the copolymers was calculated. For the copolymer $(PP\text{-}PTh)_{1.80}$, the ratio of structural units Biph/Th was 1/1, i.e. it contains equal number of structural units of Biph and Th, whereas for $(PP\text{-}PTh)_{1.84}$, the ratio was 1/1.5, i.e. it contains more structural units of Th than Biph.

As previously mentioned, the different solubility behavior of the copolymers indicates that their structure differs from that of the homopolymers. Copolymer $(PP\text{-}PTh)_{1.80}$ contains equal structural units of Biph and Th (based on EDAX), which are distributed (and not in the form of blocks, based on TGA) and it has significant crystallinity (based on XRD), indicating order between the macromolecules. Thus, it seems that the copolymer $(PP\text{-}PTh)_{1.80}$ is an alternating copolymer.

Electrical conductivity and energy gap of the copolymers

In Table VI, the electrical conductivity of the films is presented. Generally, the copolymers have one order of magnitude higher conductivity than homopolymers. The highest conductivity for polyphenylenes is

TABLE V
Energy Dispersive X-Ray Analysis (EDAX) of the Films Synthesized

Code of polymers	Elemental analysis (% w/w)				Ratio		Ratio of structural unit per counter ion	Ratio of structural units into the copolymers
	C	O	S	F	F/C (w/w)	F/S (w/w)		
$PP_{1.80}$	78.13	13.67	0	8.20	0.105		Biphenyl units 5/1	
$PP_{1.84}$	80.7	9.54	0	9.76	0.121		Biphenyl units 4.4/1	
$PTh_{1.71}$	63.05	13.75	14.00	9.22	0.146	0.658	Thiophene units 3.6/1	
$PTh_{1.75}$	64.70	13.17	13.55	8.58	0.209	0.633	Thiophene units 3.8/1	
$(PP\text{-}PTh)_{1.80}$	60.53	16.09	9.14	14.24	0.235	1.558		Biph/Th = 1/1
$(PP\text{-}PTh)_{1.84}$	61.62	9.62	14.00	14.76	0.240	1.054		Biph/Th = 1/1.5

TABLE VI
Values of E^{ox}_{onset}, E^{red}_{onset}, E_{HOMO}, E_{LUMO}, E_g of the Films and the Electrical Conductivity of Polymeric Films

Code of polymers	E^{ox}_{onset} (V)	E_{HOMO} (eV)	E^{red}_{onset} (V)	E_{LUMO} (eV)	E_g (eV)	Electrical conductivity, σ, (S/cm)
$PP_{1.80}$	+0.55	−4.95	−0.98	−3.42	1.53	2.4×10^{-2}
$PP_{1.82}$	+0.58	−4.98	−0.97	−3.43	1.55	1.3×10^{-2}
$PP_{1.84}$	+0.62	−5.02	−0.87	−3.53	1.49	6.2×10^{-1}
$PTh_{1.71}$	+0.50	−4.90	−0.95	−3.45	1.45	8.3×10^{-2}
$PTh_{1.73}$	+0.50	−4.90	−0.95	−3.45	1.45	8.0×10^{-2}
$PTh_{1.75}$	+0.50	−4.90	−0.98	−3.42	1.48	6.0×10^{-2}
$(PP\text{-}PTh)_{1.80}$	+0.71	−5.11	−0.48	−3.92	1.19	9.2×10^{-1}
$(PP\text{-}PTh)_{1.82}$	+0.80	−5.20	−0.41	−3.99	1.21	7.8×10^{-1}
$(PP\text{-}PTh)_{1.84}$	+0.60	−5.00	−0.78	−3.62	1.38	1.2×10^{-1}

E^{ox}_{onset}: Onset potential for p-doping, vs SCE.
E^{red}_{onset}: Onset potential for n-doping, vs SCE.
E_{HOMO}: Energy level of highest occupied molecular orbital (HOMO), i.e. of valence band.
E_{LUMO}: Energy level of lowest unoccupied molecular orbital (LUMO), i.e. of conduction band.
E_g: Energy gap.

exhibited in $PP_{1.84}$ (6.2×10^{-1} S/cm), i.e. the film synthesized in potential higher than E_{ox} of biphenyl (1.80 V). Similarly, the highest conductivity for polythiophenes is exhibited in $PTh_{1.71}$ (8.3×10^{-2} S/cm), again synthesized in potential higher than E_{ox} of thiophene (1.65 V). The highest conductivity for the copolymers is exhibited in $(PP\text{-}PTh)_{1.80}$ (9.2×10^{-1} S/cm), synthesized in the E_{ox} of the system of the monomers (1.80 V).

The electrical conductivity of the copolymers can be correlated to the morphology of the films and to their ratio of biphenyl to thiophene structural units (calculated from EDAX). Likewise, the electrical conductivity of the homopolymers can be correlated to the morphology of the films and to their ratio of structural units per counter ion (calculated from EDAX). For all polymers, the higher conductivity appears in the more compact films. This can be explained considering that the more compact films have a more extensive and continuous network of active paths, which facilitate the charge transfer. In homopolymers, the higher conductivity appears in polymers having the lowest ratio of structural units per counter ion, which indicates that they are more doped.[5] Considering that polythiophenes generally have lower conductivity than polyphenylenes, it can be expected that the higher content of thiophene units, the lower the conductivity of the copolymers would be. Thus, in copolymers, the higher conductivity appears in polymers having the lowest ratio of thiophene units.

The electrical conductivity can be correlated with the structure of the polymers. In polyanilines, the ratio of the peak area of quinoid to benzenoid rings (from the FTIR spectra) is a measure of their oxidation level, and it has been connected to their electrical conductivity.[51] Correspondingly, the ratios R of the peak area of the quinoid (A_{1570}) to benzenoid (A_{1480}) absorption bands of the synthesized polymers were calculated. Figure 7 presents the logarithm of electrical conductivity (logσ) of homopolymers and copolymers versus the ratio R. For the copolymers, the electrical conductivity increases by increasing R, following a linear relationship and the same behavior is also observed for the homopolymers. This confirms a direct correlation between electrical conductivity and R, i.e. the electrical conductivity increases by increasing the quinoid structures in the macromolecules.

Figure 8 shows the cyclic voltammogram of the copolymer film $(PP\text{-}PTh)_{1.84}$. The onset potentials of oxidation and reduction for the p-doping (E^{ox}_{onset}) and n-doping (E^{red}_{onset}), respectively, were determined graphically.[53,54] Then, from the equations de Leeuw et al.,[53,54] E_{HOMO}, E_{LUMO}, and E_g were calculated.

$$E_{HOMO} = -e(E^{ox}_{onset} + 4.4) \quad (2)$$

$$E_{LUMO} = -e(E^{red}_{onset} + 4.4) \quad (3)$$

$$E_g = e(E^{ox}_{onset} - E^{red}_{onset}) \quad (4)$$

where E^{ox}_{onset}: onset potential for p-doping, vs SCE

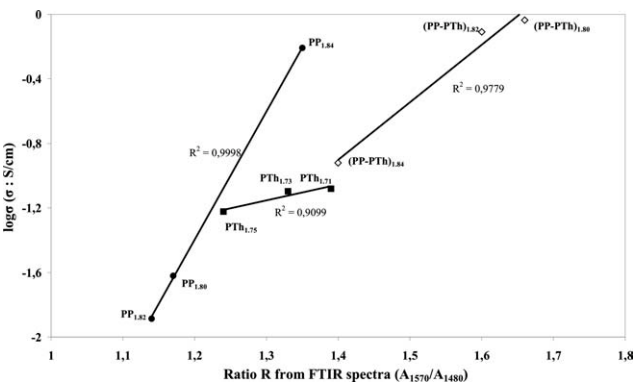

Figure 7 Electrical conductivity of polymer films versus the ratio R of the peak area of the quinoid to benzenoid (for the codes see Table I).

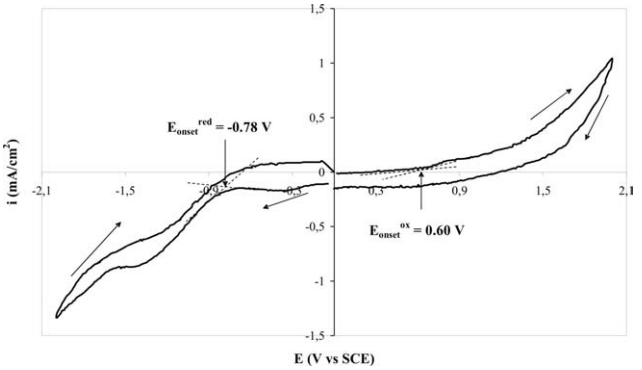

Figure 8 Cyclic voltammogram of the copolymer film $(PP\text{-}PTh)_{1.84}$ (for the code see Table I) with solution of 0.1*M* $TBABF_4$ in ACN, scan rate = 100 mV/s.

E^{red}_{onset}: onset potential for n-doping, vs SCE

E_{HOMO}: energy level of highest occupied molecular orbital (HOMO), i.e. of valence band

E_{LUMO}: energy level of lowest unoccupied molecular orbital (LUMO), i.e. of conduction band

E_g: energy gap

The values of E^{ox}_{onset}, E^{red}_{onset}, E_{HOMO}, E_{LUMO}, and E_g of the homopolymers and the copolymers are summarized in Table VI. The E_g varies from 1.19 up to 1.55 eV, i.e., the values are in the range of semiconductors.[55] E_g is reversely proportional to the electrical conductivity, thus the polymers with the higher conductivity had also the lower E_g, namely $PP_{1.84}$ (1.49 eV), $PTh_{1.71}$ (1.45 eV), and $(PP\text{-}PTh)_{1.80}$ (1.19 eV). According to the literature,[56,57] materials with values of electrical conductivity higher than 10^{-3} S/cm can be used in batteries, sensors, light-emitting diodes, etc. Thus, the copolymer films are suitable candidate materials for this kind of applications.

Stability of the synthesized films

The stability of the films under repetitive potential cycling is very important for practical applications. Cyclic voltammetry was used as a method to evaluate the stability of the copolymer films synthesized. The film (as deposited film on the electrode) was placed in a solution of ACN with $TBABF_4$ (0.1*M*) and underwent repetitive cyclic potential sweeps with a scan rate of 100 mV/s in two different potential regions (a) broad: from −2 V to +2 V, which is used for the determination of the energy gap and (b) narrow: from 0 to +2 V, which is used for many applications, such as sensors. For every cycle the anodic and cathodic peaks (i.e. their corresponding potential and current), as well as the total charge of the cycle were determined. Copolymers are very stable in both potential regions. Specifically, in the broad potential region they are stable up to 60 cycles, before their peaks begin to shift. The corresponding charge exhibited only a small decrease (0.17% per cycle with reference to the charge of the first cycle). In the narrow potential region, copolymers are even more stable, i.e. up to 250 cycles, before their peaks begin to shift slightly. The corresponding charge exhibited smaller decrease (0.024% per cycle with reference to the charge of the first cycle). Concerning the homopolymers (polyphenylenes and polythiophenes), they are profoundly less stable compared to the copolymers. Indeed, they are stable only up to 15 cycles in the broad potential region and up to 20 cycles in the narrow one.

CONCLUSIONS

New electrically conducting copolymer films were synthesized by potentiostatic electropolymerization of biphenyl with thiophene, having different structure and properties than the corresponding homopolymers. The growth of all the films follows a layer by layer (2D) mechanism. The copolymers combine high conductivity (up to 1 S/cm), low energy gap (1.2 eV), high stability under repetitive potential cycling and partial solubility, i.e. characteristics attractive for many applications such as in batteries, LEDs, sensors etc.

References

1. Guimard, N. K.; Gomez, N.; Schmidt, C. F. Prog Polym Sci 2007, 32, 876.
2. Goncalves, V. C.; Balogh, D. T. Sens Actuators 2009, 142, 55.
3. Sarac, A. S. In Encyclopedia of Polymer Science and Technology; Mark, H. F., Ed.; Wiley: New York, 2006; Vol. 6.
4. Foot, P. J. A.; Kaiser, A. B. In Kirk-Othmer Encyclopedia of Chemical Technology; Kirk-Othmer, Eds.; Wiley: New York, 2004; Vol. 7.
5. Zarras, P.; Irvin, P. In Encyclopedia of Polymer Science and Technology; Mark, H. F., Ed.; Wiley: New York, 2003; Vol.6.
6. Bobacka, J.; Ivaska, A.; Lewenstam, A. J Electroanal Chem 2003, 15, 366.
7. Maiti, J.; Pokhrel, B.; Boruah, R.; Dolui, S. K. Sens Actuators 2009, 141, 447.
8. Grimsdale, A. C.; Müllen, K. Adv Polym Sci 2006, 199, 1.
9. Aeiyach, S.; Said, A. H.; Molinié, P.; Alimi, K. Synth Met 2004, 143, 103.
10. Lacaze, P. C.; Aeiyach, S.; Lacroix, J. C. In Handbook of Organic Conductive Molecules and Polymers; Nalwa, H. S., Ed.; Wiley: Chichester, 1997.
11. Kovacic, P.; Jones, M. B. Chem Rev 1987, 87, 357.
12. Schopf, G.; Kosmehl, G. Adv Polym Sci 1997, 129, 3.
13. Roncali, J. Chem Rev 1992, 92, 711.
14. Latonen, R. M.; Kvarnström, C.; Ivaska, A. J Electroanal Chem 2001, 512, 36.
15. Latonen, R. M.; Kvarnström, C.; Ivaska, A. Electrochem Acta 1999, 44, 1933.
16. Latonen, R. M.; Kvarnström, C.; Ivaska, A. Synth Met 2002, 129, 135.
17. Latonen, R. M.; Kvarnström, C.; Grzeszczu, M.; Ivaska, A. Synth Met 2002, 130, 257.
18. Latonen, R. M.; Lönnqvist, J. E.; Jalander, L.; Kvarnström, C.; Ivaska, A. Electrochem Acta 2006, 51, 1244.
19. Latonen, R. M.; Lönnqvist, J. E.; Jalander, L.; Fröberg, K.; Kvarnström, C.; Ivaska, A. Synth Met 2006, 156, 878.

20. Aeiyach, S.; Lacaze, P. C. J Polym Sci A: Polym Chem 1989, 27, 515.
21. Blythe, A. R. Electrical Properties of Polymers; Cambridge University Press: Cambridge, 1979.
22. Udayakumar, D.; Vasudene Adhikari, A. Synth Met 2006, 156, 1168.
23. Cervini, R.; Li, X. C.; Spencer, G. W.; Holmes, A. B.; Moratti, S. C.; Friend, R. H. Synth Met 1997, 84, 359.
24. Xu, J.; Nie, G.; Zhang, S.; Han, X.; Hou, J.; Pu, S. J Mater Sci 2005, 40, 2867.
25. Freitas, M.; Duarte, M. L.; Darbre, T.; Abrantes, L. M. Synth Met 2005, 155, 549.
26. De Mattei, R. C.; Feigelson, R. S. In Electrochemistry of Semiconductors and Electronics Processes and Devices; McHardy, J., Ludwig, F., Eds.; Noyes: New Jersey, 1992.
27. Diaz, A. F.; Castillo, J. L.; Logan, J. A.; Lee, W. Y. J Electroanal Chem 1981, 129, 115.
28. Zotti, G.; Cattarin, S.; Comisso, N. J Electroanal Chem 1987, 235, 259.
29. Waltman, R. J.; Bargon, J.; Diaz, A. F. J Phys Chem 1983, 87, 1459.
30. Sari, B.; Talu, M.; Yildirim, F.; Balci, E. K. Appl Surf Sci 2002, 9493, 1.
31. Zotti, G. In Handbook of Organic Conductive Molecules and Polymers; Nalwa, H. S., Ed.; Wiley: Chichester, 1997.
32. Martion, R. E.; Peckham, T. J.; Holmes, A. B. Encyclopedia of Materials: Science and Technology; Elsevier: New York, 2001.
33. Vignali, M.; Edwards, R. A. H.; Serantoni, M.; Cunnane, V. J. J Electroanal Chem 2006, 591, 59.
34. Rajagopalan, R.; Iroh, J. O. Electrochim Acta 2002, 47, 1847.
35. Lacaze, P. C.; Hara, S.; Soubiran, P.; Aeiyach, S. Synth Met 1995, 75, 111.
36. Hillman, A. R.; Mallen, E. F. J Electroanal Chem 1987, 220, 351.
37. Soubiran, P.; Aeiyach, S.; Lacaze, P. C. J Electroanal Chem 1991, 303, 125.
38. Bade, K.; Tsakova, V.; Schultze, J. W. Electrochim Acta 1992, 37, 2255.
39. Scharifker, R. B.; Hills, G. Electrochim Acta 1983, 28, 879.
40. Wallace, G. G.; Spinks, G. M.; Kane-Maguire, L. A. P.; Teasdale, P. R. Conductive Electroactive Polymers, Intelligent Materials Systems, 2nd ed.; Taylor & Francis: Boca Raton, 2003.
41. Downard, A. J.; Pletcher, D. J Electroanal Chem 1986, 206, 139.
42. Simitzis, J.; Triantou, D.; Soulis, S. J Appl Polym Sci 2008, 110, 356.
43. Simitzis, J.; Dimopoulou, C. Makromol Chem 1984, 185, 2553.
44. Simitzis, J.; Zoumboulakis, L.; Stamboulis, A.; Hinrichsen, G. Angew Makromol Chem 1993, 213, 181.
45. Simitzis, J.; Tzevelekis, D.; Stamboulis, A.; Hinrichsen, G. Acta Polym 1993, 44, 294.
46. Hotta, S. In Handbook of Organic Conductive Molecules and Polymers; Nalwa, H. S., Ed.; Wiley: Chichester, 1997.
47. Vatansever, F.; Hacaloglu, J.; Akbulut, U.; Toppare, L. Polym Int 1996, 41, 237.
48. Wang, X.; Shi, G.; Liang, Y. Electrochem Comm 1999, 1, 536.
49. Furukawa, Y.; Akimoto, M.; Harada, I. Synth Met 1987, 18, 151.
50. Akimoto, M.; Furukawa, Y.; Takeuchi, H.; Harada, I. Synth Met 1986, 15, 353.
51. Bhadra, S.; Singha, N. K.; Khastgir, D. J Appl Polym Sci 2007, 104, 1900.
52. Sestrem, R. H.; Ferreira, D. C.; Landers, R.; Temperini, M. L. A.; do Nascimento, G. M. Polymer 2009, 50, 6043.
53. Li, Y.; Cao, Y.; Gao, J.; Wang, D.; Yu, G.; Heeger, A. J. Synth Met 1999, 99, 243.
54. Burghard, M.; Fischer, C. M.; Roth, S.; Schlick, U.; Hanack, M. Synth Met 1996, 76, 241.
55. Neamen, D. A. Semiconductor Physics and Devices: Basic Principles; 3rd ed.; Mc Graw Hill: Boston, 2003.
56. Smyrl, W. H.; Lien, M. In Applications of Electroactive Polymers; Scrosati, E. B., Ed.; Chapman & Hall: London, 1993.
57. Furukawa, N.; Nishio, K. In Applications of Electroactive Polymers; Scrosati, E. B., Ed.; Chapman & Hall: London, 1993.